Self-Gravity, Perturbations, and Magnetic Fields in Gamma-Ray Burst Progenitors

Piotr Płonka[1]

Agnieszka Janiuk[2]

[1]Astronomical Observatory of the University of Warsaw

[2]Center for Theoretical Physics PAS

Thursday, April 3, 2025

Presentation Outline

1. Introduction to Gamma-ray bursts
2. Why Do We Need Supercomputers?
3. Results
4. Conclusions

History of Gamma-ray bursts

- The history of gamma-ray bursts began in the 1960s with the launch of the Vela satellites.

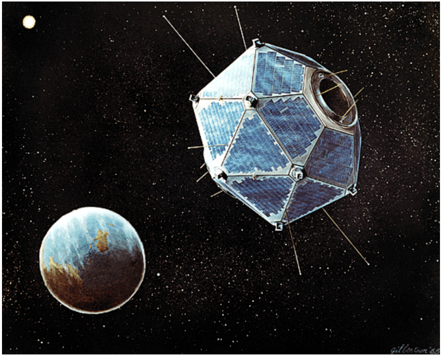

Figure 1: Artist's impression of Vela 5B satellite in orbit.

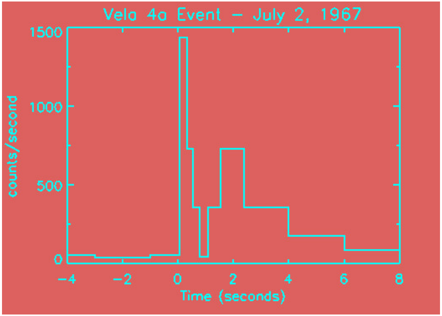

Figure 2: Lightcurve of the first GRB detected by the military satellites Vela 3 and 4.

History of Gamma-ray bursts

- Gamma-ray bursts are distributed **isotropically**.
- Afterglows are necessary to measure the **redshift** and **distance**.
- GRBs are the most energetic electromagnetic sources in the Universe.

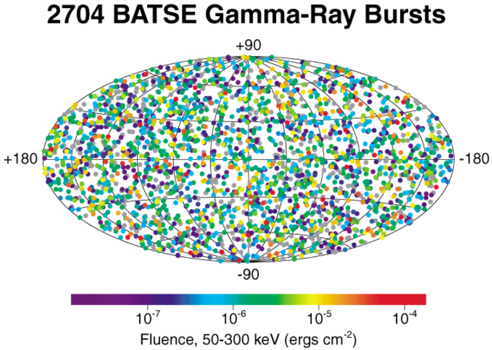

Figure 3: The map shows burst locations in galactic coordinates.

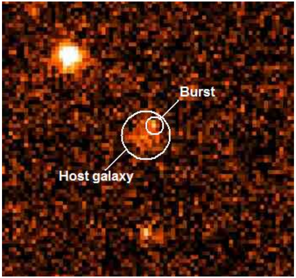

Figure 4: GRB 970228 was the first gamma-ray burst for which an afterglow was observed.

Two types of Gamma-ray bursts

- Gamma-ray bursts (GRBs) are classified into two categories:
  - **Long GRBs** (> 2 s)
  - **Short GRBs** (< 2 s)

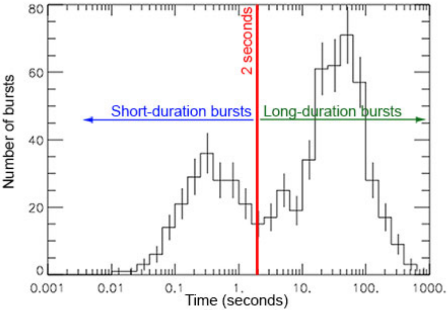

Figure 5: GRBs observed by the BATSE instrument on the Compton Gamma-ray Telescope.

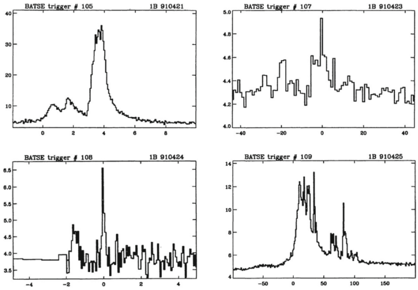

Figure 6: Despite the classification into short and long GRBs, each burst is unique.

Two types of Gamma-ray bursts

Gamma-ray bursts are classified into two categories:

- **Long GRBs** are associated with **the collapse of massive stars**.
- **Short GRBs** are associated with **mergers** of compact objects.

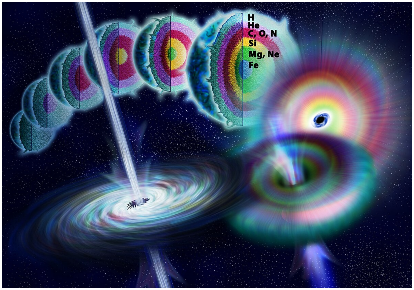

Figure 7: Collapse of a massive star.

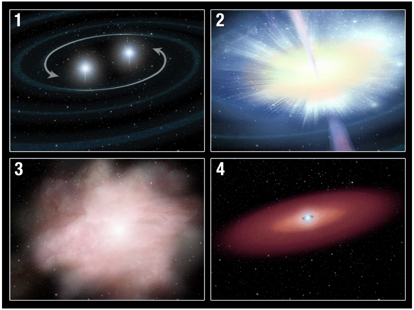

Figure 8: Merger of neutron stars.

Long Gamma-ray Bursts

- They originate from the collapse of massive, rotating stars, which leads to the formation of a rapidly spinning black hole.
- Modeling these phenomena requires considering a **relativistic**, **highly magnetized** fluid within the framework of **general relativity**.

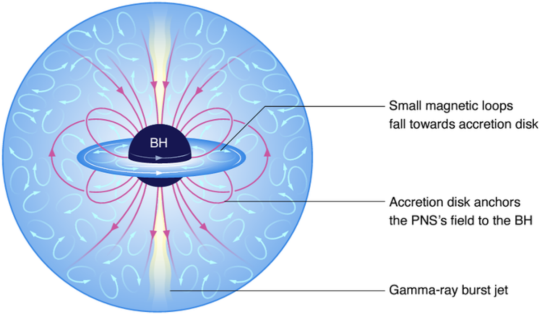

Figure 9: Mass accretion onto a newly born black hole.

- **HARM** solves **hyperbolic** equations using the **finite-volume method**. The code works on **CPUs** with **MPI** .
- The code solves three equations: the continuity equation, the conservation of energy and momentum, and the evolution of the magnetic field:

$$\nabla_\mu(\rho u^\mu) = 0, \quad \nabla_\mu T^\mu_\nu = 0, \quad \nabla_\mu(u^\mu b^\nu - u^\nu b^\mu) = 0. \tag{1}$$

- Additionally, using the CT (constrained transport) method ensures that:

$$\nabla \cdot \vec{B} = 0 \tag{2}$$

- The complete stress–energy tensor is expressed as:

$$T^{\mu\nu}_{\mathrm{MHD}} = (\rho + u + p + b^2)u^\mu u^\nu + \left(p + \frac{1}{2}b^2\right) g^{\mu\nu} - b^\mu b^\nu. \tag{3}$$

A Numerical Scheme for GRMHD

1. Initialize the grid and assign the primitive variables P to the grid cells.

$$P = (\rho, u, u^1, u^2, u^3, B^1, B^2, B^3) \tag{4}$$

2. Interpolate the primitive variables at the cell edges P_L and P_R, using a linear slope limiter (MINMOD).
3. Calculate the conserved variables U from P (analytically):

$$U = \sqrt{-g}(\rho u^0, T^0_0, T^0_1, T^0_2, T^0_3, B^1, B^2, B^3) \tag{5}$$

4. Calculate the HLLE fluxes:

$$F_{i+\frac{1}{2}} = \frac{c_{\mathrm{min}} F_R + c_{\mathrm{max}} F_L - c_{\mathrm{max}} c_{\mathrm{min}} (U_R - U_L)}{c_{\mathrm{max}} + c_{\mathrm{min}}} \tag{6}$$

5. Evolve the conserved variables with additional source terms due to curved spacetime:

$$\partial_t U(P) = \partial_i F_i(P) + S(P) \tag{7}$$

A Numerical Scheme for MHD with Self-Gravity

6. Evolve the magnetic field using the constrained transport (CT) method.
7. Evolve the metric (a and M_{BH}) due to self-gravity and black hole event horizon crossing, for mass:

$$\Delta M(t) = \int_0^t \int_0^{2\pi} \int_0^{\pi} \sqrt{-g}\, T_t^r \, d\theta \, d\phi \, dt' \tag{8}$$

$$\delta M(t,r) = \int_{r_g}^r \int_0^{2\pi} \int_0^{\pi} \sqrt{-g}\, T_t^t \, d\theta \, d\phi \, dr'. \tag{9}$$

$$M(t,r) = M_0 + \Delta M(t) + \delta M(t,r). \tag{10}$$

Reconstruction of Primitive Variables from Conserved Variables:

8. Using the Newton-Raphson method, solve 5 nonlinear equations to compute P from U. **This is the core of HARM.**

Models

Our goals:

- For the first time, we study the influence of self-gravity in **three-dimensional** models. We compare the evolution of the system - with and without self-gravity - under different initial conditions, including **magnetic field configuration** and **strength**, **internal energy perturbations**, black hole **mass** and **spin**, as well as envelope **mass** and **angular momentum**.

- The resolution of models is **256x128x64** = **2 097 152** cells.
- Twelve models were computed (6 with and 6 without SG).

Model	**CPU Hours**
With self-gravity	$\approx$ 70,000
Without self-gravity	$\approx$ 40,000

Table 1: Comparison of computational requirements for one model on the ARES supercomputer using 32-node calculations.

Magnetic Field Configurations

- We used two magnetic field configurations: **vertical** and **hybrid**.

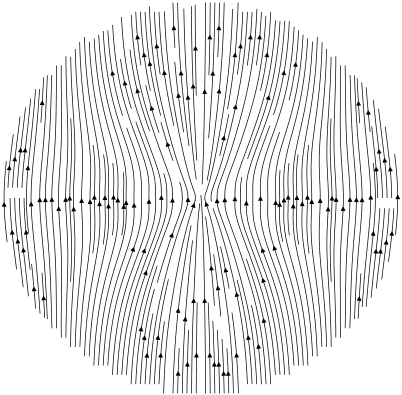

(a) Vertical

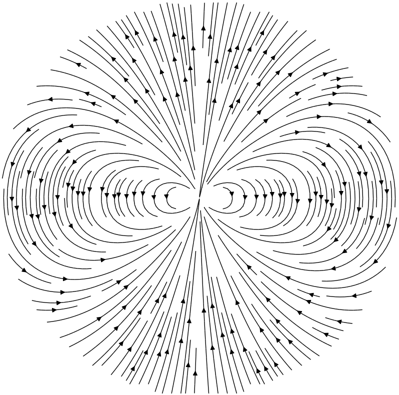

(b) Hybrid

Accretion rate

- Models with self-gravity exhibit **greater variability** in the accretion rate, which is more consistent with observations of prompt gamma-ray burst emissions.

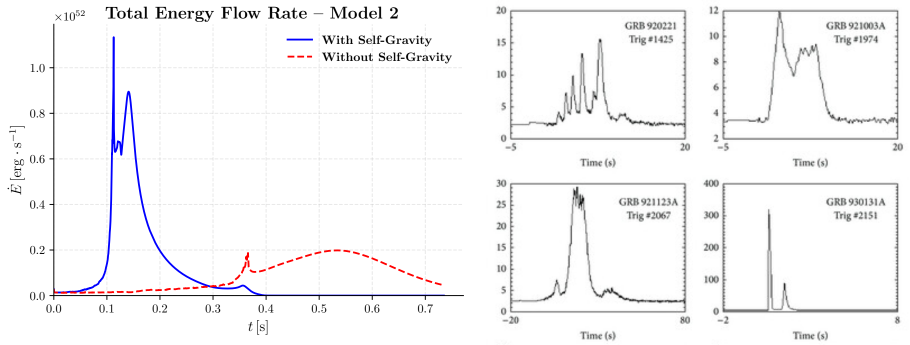

Figure 11: Energy accretion rate $\dot{E}$ for models with and without self-gravity under identical initial conditions (left) and observed prompt emission from GRBs (right).

- Models with self-gravity evolve **faster** than models without self-gravity.

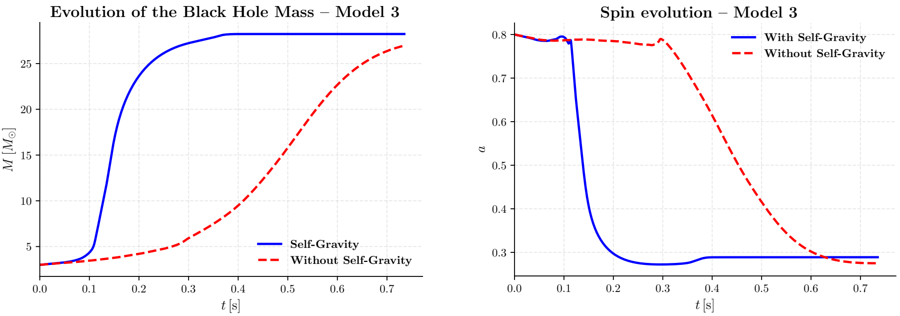

Figure 12: Evolution of the black hole mass M_{BH} (left) and the spin parameter a (right) for models with and without self-gravity.

Pressure inhomogeneities

- In the self-gravity models, **pressure instabilities** emerge when the energy accretion rate is the highest. Notice also that perturbations are more clearly visible in the model without self-gravity.

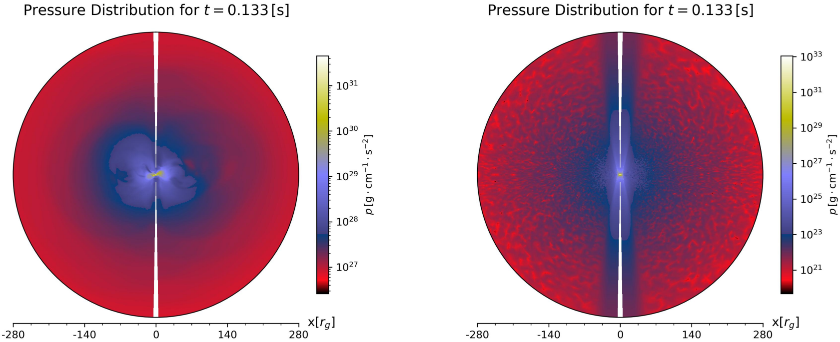

Figure 13: Comparison of non-self-gravitating (left) and self-gravitating (right) cases, evolved from the same initial conditions.

Jet Formation under Self-Gravity

- This is the first study to explore the formation of jets in the context of self-gravity effects.

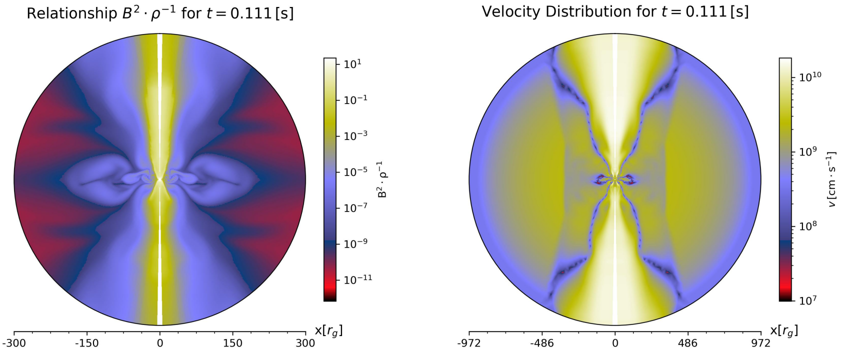

Figure 14: The polar slices showing the jet.

Spiral structures under Self-Gravity

- The creation of spiral structures in self-gravity and non-self-gravity models can be compared using **3D** simulations.

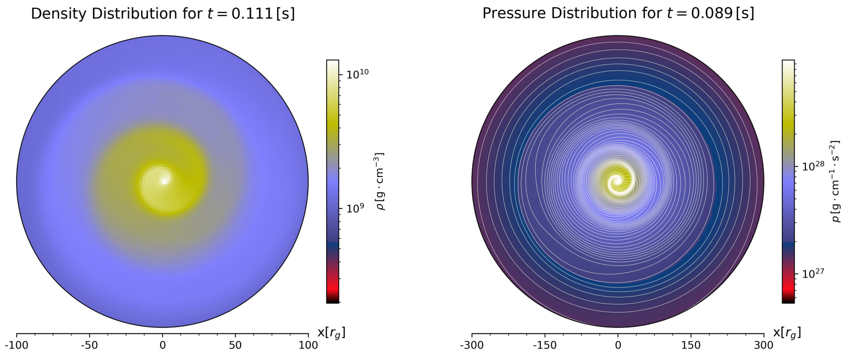

Figure 15: The equatorial slices demonstrate the presence of spiral structures.

Conclusions

- Three-dimensional General Relativistic Magnetohydrodynamical simulations are **computationally expensive**.
- The evolution of the black hole's spin and mass is both quantitatively and qualitatively **affected by self-gravity**, confirming the findings from our previous 2D studies.
- In the self-gravity models, **pressure instabilities appear** when the energy accretion rate is the highest.
- The **accretion rate variability** is stronger in self-gravitating collapsars and may produce detectable signals in GRB prompt emission.
- **3D** dimensional models, even though computationally expensive, show more details about astrophysical processes.

Thank You for Your Attention!